

**Modeling of Transition State in Grignard Reaction of Rigid N-(Aryl)imino-Acenaphthenone (Ar-BIAO):
An Experimental and Computational Approach**

A Project Report

Submitted to the Department of Chemistry
Indian Institute of Technology, Hyderabad
As part of the requirements for the degree of

Master of Science

By

Sayak Das Gupta

Roll No: CY12M1017

Under the supervision of

Dr. Tarun K. Panda



भारतीय प्रौद्योगिकी संस्थान हैदराबाद
Indian Institute of Technology Hyderabad

DEPARTMENT OF CHEMISTRY
INDIAN INSTITUTE OF TECHNOLOGY, HYDERABAD

April, 2014

Declaration

I hereby declare that the matter embodied in this report is a result of investigation carried out by me in the Department of Chemistry, Indian Institute of Technology Hyderabad under the supervision of **Dr. Tarun K. Panda**.

In keeping with general practice of reporting scientific observations, due acknowledgment has been made wherever the work described is based on the findings of other investigators.

Sayak Dasgupta

(Signature)

Sayak Das Gupta

(Student Name)

Tarun Kantu Panda

Signature of the supervisor

CY12M1017

(Roll No)

Approval Sheet

This thesis entitled “**Modeling of Transition State in Grignard Reaction of Rigid N-(Aryl)imino-Acenaphthenone (Ar-BIAO): An Experimental and Computational Approach**” by Sayak Das Gupta is approved for the degree of Master of Science from IIT Hyderabad.

Name and affiliation-
Examiner

Name and affiliation-
Examiner

Name and affiliation-
Adviser

Name and affiliation-
Co-Adviser

Name and affiliation-
Chairman

Acknowledgements

The completion of my M.Sc. project would not have been possible without the kind support and help of many individuals. I would like to extend my sincere thanks to all of them.

I express my deep sense of gratitude to my thesis supervisor Dr. Tarun K. Panda who guided me in my every possible aspect of my project from the very beginning and played a pivotal role in suggesting and helping me to develop ideas for this project. He has been a constant source of moral support and encouragement, especially during the difficult times. I would like to thank him once again for being patient with me while clearing all my doubts. Thank you Sir.

I would like express my sincere thanks to Dr. Bhabani S. Mallik for helping to learn, understand and apply computational chemistry which has played a crucial role in my project. He was always available for discussion whenever I faced difficulties.

I would like express my gratitude towards the research scholars in our group: Mr. Ravi Kotallanka, Mr. Kishor Naktode, Mr. Srinivas Anga,, Mr. Harinath Adimullam., Ms. Jayeeta Bhattacharjee for their constant guidance and suggestions in different aspects of the project.

I would like to thank my fellow M.Sc. group members Ms. Abhinanda Kundu and Mr. Supriya Rej for their constant support and also express gratitude towards all my fellow classmates who motivated me to carry on.

I would like to acknowledge “High Performance Computing” at IIT Hyderabad.

I am thankful to the Department of Chemistry, IIT Hyderabad for helping me in various ways.

Lastly, I offer my regards to all of those who supported me in any respect during the completion of the project.

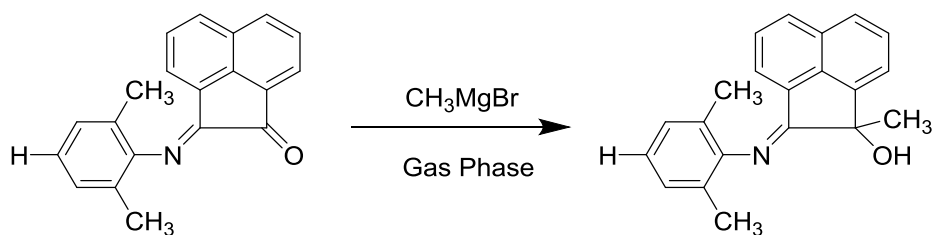
Dedicated
To
My Parents

Contents

Abstract:	7
Chapter 1: Modeling of Transition State in Grignard Reaction of Rigid <i>N</i> -(Aryl)imino-Acenaphthenone (Ar-BIAO): An Experimental and Computational Approach	
1.1 Introduction	10
1.2 Scope of the work	12
1.3 Computational Methodology	13
1.3.1 Computational Study.....	15
1.4 Results and Discussion	16
1.4.1 Experimental Study.....	16
1.4.2 Chelation vs Non-Chelation Coordination.....	18
1.4.3 Model System	19
1.4.4 Real System	23
1.5 Conclusion	25
References.....	26
Chapter 2: Basicity of <i>Imidazolin-2-ylidene-1,1-diphenylphosphinamine</i> and Analogous Systems-A Computational Study	
2.1 Introduction.....	29
2.2 Scope of the work	30
2.3 Methodology	31
2.4 Results and Discussion:	32
2.5 Conclusion	40
References:.....	41

Abstract:

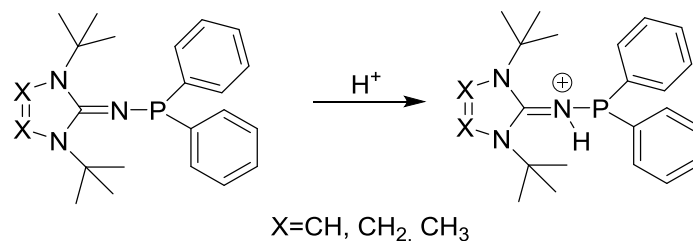
In chapter 1, a combined synthetic and computational study has been carried out on the addition of Grignard reagents RMgBr (R = Me, Et) to various sterically rigid *N*-(Aryl)imino-Acenapthenone (Ar-BIAO) (Ar = 2,6-ⁱPr₂C₆H₄ (**1**), 2,6-Me₂C₆H₄ (**2**), 2,4,6-Me₃C₆H₃ (**3**) ligands. In the experimental method, when the compounds **1-3** were treated with RMgBr (R = Me, Et) in ambient temperature, the corresponding *N*-(Aryl)imino-Acenaphthylene-1-ol (Ar-BIAOH) (Ar = 2,6-ⁱPr₂C₆H₄; R = Me (**1a**), Et (**1b**); Ar = 2,6-Me₂C₆H₄; R = Me (**2a**), Et (**2b**) and Ar = 2,4,6-Me₃C₆H₃; R = Me (**3a**), Et (**3b**) were obtained in a yield up to 82%. The Ar-BIAOH compounds were characterized by spectroscopic and combustion analyses and the solid state structures of the compounds **1a-3a** were established by single crystal X-ray diffraction analysis. To model the transition state of the Grignard reaction with unsymmetrical and sterically rigid Ar-BIAO ligands having three fused rings containing exocyclic carbonyl and imine functionality, we carried out computational analysis. During our study, we have considered the gas phase addition of CH₃MgBr to **2** (Scheme a) and the model system of 2-(methylimino)pentanone (**2'**). We have carried out *ab-initio* (HF/3-21G(d)) and density functional theory (DFT) calculations with the hybrid density functional B3LYP/6-311+G(2d,p) to probe into two major aspects (i) stability of an intra-molecular chelation involving Magnesium, carbonyl Oxygen and imine Nitrogen (ii) to suggest a probable transition state and mechanistic pathway. The theoretical analysis suggests the formation of tetra-coordinated magnesium complex as the transition state.



Scheme a: Gas phase reaction to be investigated by computational methods

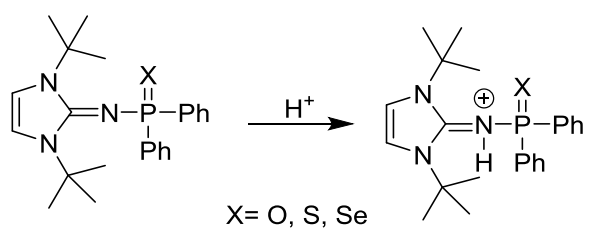
In the second part of the thesis work DFT calculations have been performed to optimize *1,3-di-tert-butyl-N-(diphenylphosphino)-1H-imidazol-2(3H)-imine* (**1**) and its corresponding sulphur and selenide derivative and it was observed that the resulting calculated geometries were in excellent agreement with those established by X-ray Diffraction analyses. To further analyze the

properties and electronic structure, the protonation energies (Scheme b) of compound **1**, model system (1,3-di-tert-butyl- N(diphenylphosphino)imidazolin-2-imine) (**1'**) and 1,3-di-tert-butyl-1,3-dimethyl-2-(diphenylphosphino)guanidine) (**1''**) have been calculated by means of density functional theory.



Scheme b: Protonation of ligands **1**, **1'** and **1''**.

Finally the charge distribution has been determined for compounds **1**, **1'** and **1''** using Natural Bond Orbital (NBO) analysis. From the charge distribution it was realized the exocyclic nitrogen having the highest negative charge is most likely to get protonated. Also DFT analysis provided further insight into the stabilization of a positive charge by the imidazolin ring. Furthermore to get an insight into the changes in the electronic environment around exocyclic nitrogen with different chalcogenide derivatives of ligand **1**, we computationally probed the basicity of oxygen, sulphur and selenide derivative of ligand **1** (Scheme c).



Scheme c: Protonation of chalcogenide derivatives of ligand **1**.

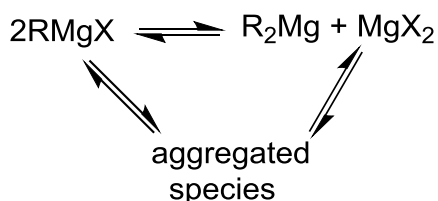
Chapter 1

Modeling of Transition State in Grignard Reaction of Rigid *N*-(Aryl)imino-Acenaphthenone (Ar-BIAO): An Experimental and Computational Approach

1.1 Introduction

With over a 100 year old history, the Grignard reaction is one of the most potent methods for C-C bond formation¹. Its importance and widespread application was realized soon after its discovery in 1900 and resulted in Victor Grignard receiving the Nobel Prize in 1912. Most of the Grignard reagents (RMgX) are easily prepared by the reaction of organic halides RX (X=Cl, Br, I) with activated Mg metal in ether or THF solvent. The basic reaction involves addition of RMgX across C=O double bond in aldehydes and ketones to form secondary and tertiary alcohols respectively. The frequent use of the Grignard reagent in several natural product syntheses² and metal-catalyzed reactions³ reflects its synthetic utility. Furthermore its application continues to evolve with time as modern day synthetic chemists explore the applications of the Grignard reagents in several homo and cross coupling reaction⁴.

Due to its immense utility the mechanism and structure of Grignard reagents has been constantly under the scanner through synthetic, X-ray analyses, spectroscopic and computational methods⁵⁻⁶. The complicacy of the mechanism arises from the wide number of possibilities depending upon the solvents used, alkyl group of the Grignard reagent and several other factors. The Grignard reagent commonly represented as RMgX, exists in solution in several complex forms, the most common one represented by the Schlenk equilibrium (Scheme 1)⁷ established by Wilhelm Schlenk, whereas in ether solvents RMgX.2Et₂O has been established as one of the most stable forms of the Grignard reagent⁸.



Scheme 1: Species in the Schlenk equilibrium

However the exact structural form of the Grignard reagent in solution continues to intrigue chemists as several *ab-initio* and density functional theory calculations have been reported to ascertain the stability of the different suggested forms of the RMgX⁹⁻¹⁰.

There have been several reports on theoretical studies carried out on the addition of Grignard reagent to α - and β -alkoxy carbonyls considering Cram chelation model¹¹ and the Felkin-Anh¹²

model as the two possible pathways. While Cram's model considers the approach of the nucleophile from the less hindered site of the double bond, Felkin-Anh's Model assumes a reactant like transition state and takes into account torsional strain in partial broken or formed bonds. There has been constant investigation based on these two models with respect to addition of organometallic reagents across C=O double bonds¹³. *Ye et al.*¹⁴ reported Grignard reaction in α -alkoxy carbonyls going through chelated as well as non-chelated intermediate in two substrates differing in their steric constraints (Figure 1).

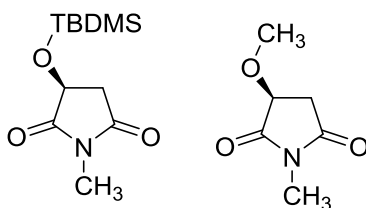
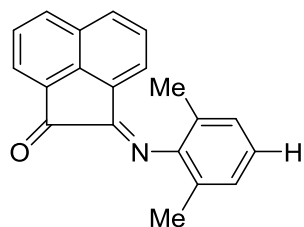


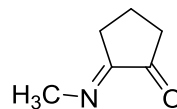
Figure 1: α -alkoxy carbonyls differing in steric constraints.

Ar-BIAO¹⁵⁻¹⁷ ligands reported by our group bear α -imino carbonyl functionality. Thus on addition of RMgX there is a possibility of both imine nitrogen and carbonyl oxygen simultaneously coordinating to the central magnesium atom to stabilize the Grignard reagent. Hence based on these studies we were interested to investigate the possibility of intramolecular chelation of magnesium atom with carbonyl oxygen and the exocyclic imine nitrogen α to the carbonyl carbon.

In the course of the reaction, where experimental isolation of an intermediate seemed very difficult as the reaction was highly spontaneous and the lifetime of the intermediate was very short. Even under inert conditions several attempts to isolate the short-lived intermediate did not meet with much success. Thus structural analysis and characterization of the intermediate which was of high interest due to the unsymmetrical nature of the ligand could not be performed experimentally, so computational study was conducted on Grignard reaction considering Ar-BIAO ligand **2** and the model system (**2'**) as the substrates (Figure 2).



(2,6-dimethylphenylimino)acenaphthylen-1(2H)-one



2-(methylimino)cyclopentanone

Figure 2: (2 and 2') Real and Model system selected for computational investigation

The rigid three ring fused system of imino-acenaphthenone and the bulky aryl group makes the system highly sterically constrained. To the best of our knowledge, there have not been much mechanistic studies of Grignard reaction on such geometrically constrained systems, which has inspired us to probe into the probable transition states and mechanisms of reactions involving addition of RMgX to Ar-BIAO ligands. Furthermore to ascertain the influence of the steric bulk on different mechanistic aspects, computational studies were carried out on the model system 2' ((2-methylimino)cyclopentanone)) which mimics the fundamental functional moiety of Ar-BIAO ligands, but instead of a rigid acenaphthenone ring it contains a much less steric cyclopentanone ring system.

1.2 Scope of the work

Due to the spontaneous nature of the reaction all our efforts to isolate an intermediate were unsuccessful. Hence we focused to carry out Density Functional Theory (DFT) calculations to understand the coordination behavior in Ar-BIAO-Mg(Br)(CH₃) intermediate and to get a better insight into the most probable transition state and mechanistic pathway. As experimentally observed, the Grignard reagent preferentially adds across the more electronegative carbonyl oxygen than the imine nitrogen which was confirmed by the shorter Mg---O bond as compared to the Mg---N bond in the intermediate suggested by computational studies. However due to the unsymmetrical nature of the ligand and the presence of two coordinating sites (oxygen and nitrogen atom) we were motivated to probe the possibility of the intramolecular chelation involving the magnesium of the Grignard reagent. Computational studies were carried out on the Ar-BIAO ligand 2 which contained a moderately steric moiety of 2,6-dimethylphenyl at the exocyclic imine nitrogen. Apart from the electronic factors, we realized that the steric factors

would also play an important role in the course of the reaction due to the rigid three membered ring and the bulky aryl substituent at the imine nitrogen. Thus it was of interest to investigate the probable intermediate and mechanism by considering a less sterically hindered model system of 2-(methylimino)pentanone (**2'**) which exhibited similar electronic behavior to that of ligand **2**.

1.3 Computational Methodology

Computational chemistry has carved its niche as one of the most important and fundamental tools of modern day chemistry. Quantum mechanical calculations have been constantly striving to corroborate between theoretical results and experimental data and thus have found extensive application in several fields of chemistry. While the Schrödinger equation can be solved accurately and conveniently for small systems, however as we move to larger systems we have to resort to certain approximations. The highly accurate first principle methods are only possible for small systems and empirical or semi-empirical methods have to be used as we try to perform quantum mechanical calculations on systems with large no of atoms.

Both first-principle and semi-empirical approaches involve approximations ranging from simplifying mathematical equations to limiting the size of the system. Semi empirical methods are usually generalizations of earlier successful π -electron methods. While first-principle or *ab-initio* methods generate accuracy by using extensive basis sets or higher levels of electron correlation, in semi-empirical methods parameters are adjusted to implicitly include electron correlation. Certain approximations are also used in *ab-initio* calculations, one of the most common one being the Born-Oppenheimer Approximation which assumes that the nuclei remains stationary during the calculation. Quantum Mechanical Calculations always aim to maintain the perfect balance between approximations and accuracy. However wave function based first principle calculations for large complicated systems is often time-consuming and computationally not cost effective. Another approximate method Density Functional Theory (DFT) has produced excellent results in such situations.

DFT has become one of the most promising tools in recent years for quantum chemistry calculations, being computationally less intensive than other methods with similar accuracy. Unlike other quantum mechanical methods like Hartree-Fock, DFT makes use of $\rho(\mathbf{r})$ [electron density] and not $\Psi(\mathbf{r})$ [wave function]. The original theory was suggested by Hohenberg and

Kohn and a practical application of this theory was developed by Kohn and Sham. In the well-known Kohn and Sham equations the potential experienced by an electron was expressed as a function of the electron density¹⁹. Scientist Walter Kohn won the Nobel Prize for Chemistry in 1998 for his contribution to the development of Density Functional Theory.

The Kohn-Sham expression for the electronic energy functional can be expressed as:

$$E[\rho] = T[\rho] + E_{eN}[\rho] + E_{ee}[\rho] + E_{xc}[\rho]$$

Where $T[\rho]$ is the kinetic energy, $E_{eN}[\rho]$ is the electron nuclear attraction, $E_{ee}[\rho]$ is the Coulombic electron – electron repulsion and $E_{xc}[\rho]$ is the exchange correlation energy.

Electron-electron correlation is one of the most important parameters in quantum chemical calculations. On solving the Schrödinger equation for He atom without considering any correlation terms, the energy value obtained shows a deviation of 38% from the experimental value. While in Hartree Fock Theory each electron sees an average charge cloud due to other electrons, in DFT certain approximations are used to calculate this correlation energy. The exchange energy is also calculated using approximations, including considering a percentage of the exchange from HF theory. Based on the approximations used there are different density functionals, the most common one being B3LYP which is a hybrid functional (containing a partial HF exchange and a General Gradient Approximated (GGA) correlation term).

Computational studies have been carried out using both *ab-initio* and DFT methods to optimize and calculate energetics of different chemical species under consideration. All calculations have been carried out with Gaussian 09²⁰ suite of programs. For visualization of optimized geometries and analysis of computational results Gauss View²¹ package has been used.

Quadratic Synchronous Transit (QST)²² approach in Gaussian 09 has also been used to predict transition states. QST 2 with two molecule specifications (reactant and product) and QST 3 with three molecule specifications (reactant, product and a guess transition state) can be used to computationally locate a transition state. QST seems superficially similar to Linear Synchronous Transit (LST) algorithm which searches for a maximum along the linear path between the reactants and the products. However LST often leads to a structure with two or more negative frequencies, thus QST which searches for maxima in the parabola connecting the reactants and the products is an improvement on LST²³.

To reduce the cost of computation, the procedure of calculating single point energies using B3LYP/6-311+G(2d,p)²⁴ on structures optimized at a lower level (HF/3-21G(d)) has been

followed, since B3LYP functional is usually insensitive to the geometry optimization level ²⁵. Unless otherwise specified, the reported energies include B3LYP single point energy with zero point energy corrections from the HF method, since this method compared to the compared to the experimental results of the so called G2-molecule set has a reasonable maximum absolute deviation value.

1.3.1 Computational Study

As several attempts to experimentally isolate the intermediate of the Grignard reaction with Ar-BIAO class of ligands were unsuccessful, the gas phase reaction of CH_3MgBr with **2** and **2'** was investigated to suggest a probable intermediate and mechanism. To get a better insight on the role of steric constraints in the reaction pathway, model system **2'** has been chosen in such a way that it contains the α -imino carbonyl functionality which is inherent to all Ar-BIAO ligands, however a methyl substituent instead of an aryl group at the nitrogen atom and presence of a simple cyclopentanone ring relieves **2'** from much of the geometrical constraints. CH_3MgBr coordinating to ligand **2** and **2'** have been considered as the pre-complex **R** and **R'** for the real and model system (Figure 3) respectively and all energies have been calculated with respect to the pre-complex.

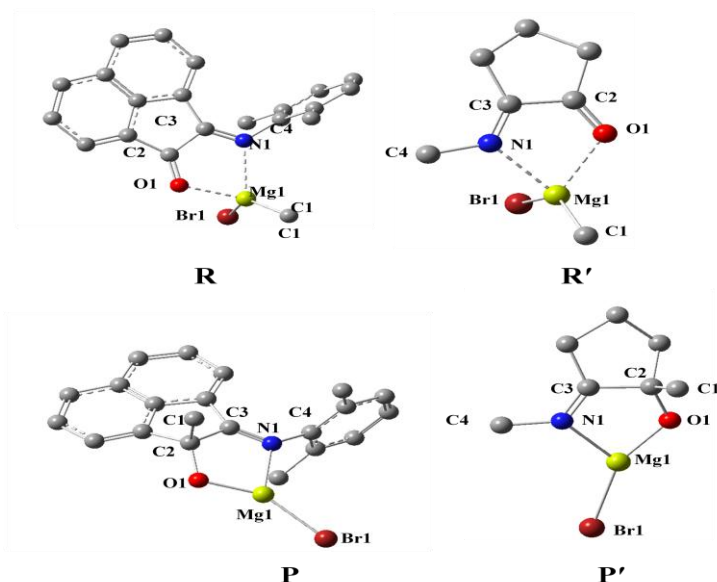


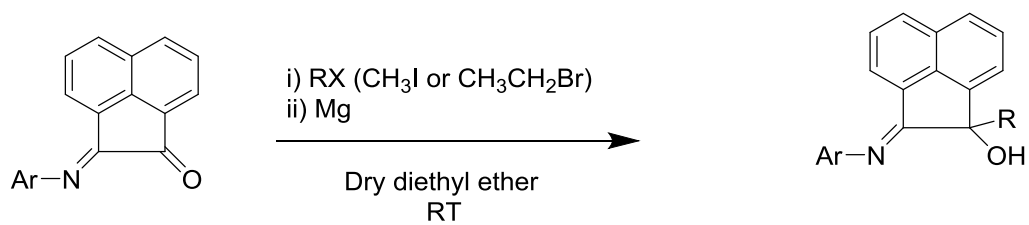
Figure 3: Optimized figures for pre (**R'**, **R**) and post-complexes (**P'**,**P**) of model and real systems.

The pre-complex (**R** & **R'**) and the post-complex (**P** and **P'**) were freely optimized without any geometrical constraints, and there occurred a decrease in the Mg1-N1 bond distances in the optimized figures as compared to the input structures, which was indicative of both nitrogen and oxygen simultaneously coordinating to magnesium. Initially our attempt to optimize a guess input structure to a transition state was unsuccessful, so we scanned the carbonyl carbon (**C1**) and the methyl carbon of the Grignard reagent (**C2**) bond without any symmetry restrictions, at the HF/3-21G(d) level to perform a series of energy minimizations where the C1-C2 bond length was varied at regular intervals and the boundary limits were the C1-C2 bond lengths in the post and pre-complex optimized structures. The probable high energy transition state was evident from the plots obtained and the energies of the TS were calculated by the combined method mentioned above. To check the accuracy of our methodology, QST2 calculations (without a guess transition state) were performed to interpolate TS between the pre and post-complex. The exact same methodology was followed for the real and the model system. The transition states were characterized by one single imaginary frequency, which on visualization was the vibration between the forming C-C bond that is the C1-C2 bond.

1.4 Results and Discussion

1.4.1 Experimental Study

Addition of Grignard reagents (CH_3MgI and $\text{C}_2\text{H}_5\text{MgBr}$) was carried out across three Ar-BIAO ligands (**1**, **2** and **3**) in dry ether solvent at room temperature (Scheme 2)¹⁸ to yield corresponding six different *N*-(aryl)imino-acenaphthylene-1-ol (Ar-BIAOH) in yields upto 82 %. All six Ar-BIAOH ligands were obtained in the racemic form (Figure 4). The Ar-BIAOH compounds were characterized by spectroscopic and combustion analyses and the solid state structures of the compounds **1a-3a** were established by single crystal X-ray diffraction analysis.



Ar = 2,6-*i*Pr₂C₆H₃ (**1**)
 = 2,6-Me₂C₆H₃ (**2**)
 = 2,4,6-Me₃C₆H₂ (**3**)

Compound	Ar	R	Yield
1a	2,6- <i>i</i> Pr ₂ C ₆ H ₃	Me	79%
1b	2,6- <i>i</i> Pr ₂ C ₆ H ₃	Et	74%
2a	2,6-Me ₂ C ₆ H ₃	Me	71%
2b	2,6-Me ₂ C ₆ H ₃	Et	79%
3a	2,4,6-Me ₃ C ₆ H ₂	Me	82%
3b	2,4,6-Me ₃ C ₆ H ₂	Et	71%

Scheme 2: Grignard Reaction on Ar-BIAO ligands.

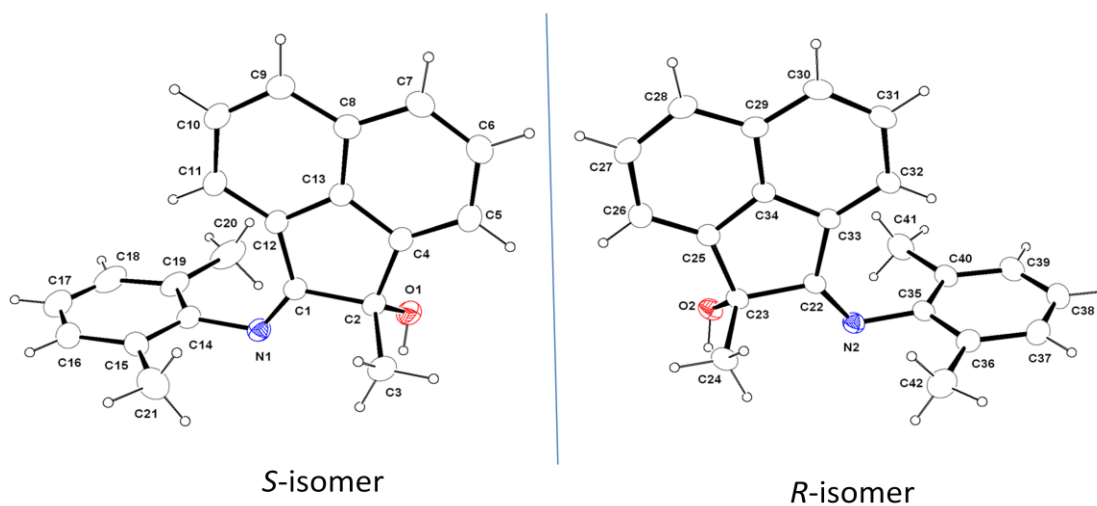


Figure 4: Solid state structure of R and S isomer of **2**.

1.4.2 Chelation vs Non-Chelation Coordination

For the pre-complex **R'** two possibilities were considered and optimized. In one of the optimized geometries the imine nitrogen was coordinating with the Mg (Mg1-N1=2.22 Å) and in the other situation there was negligible interaction between these two atoms (Mg1-N1=4.63 Å) (Figure 5). The structure with intra-molecular chelation between Mg and N was stabilized by -13.81 kcal/mol compared to the non-chelated one.

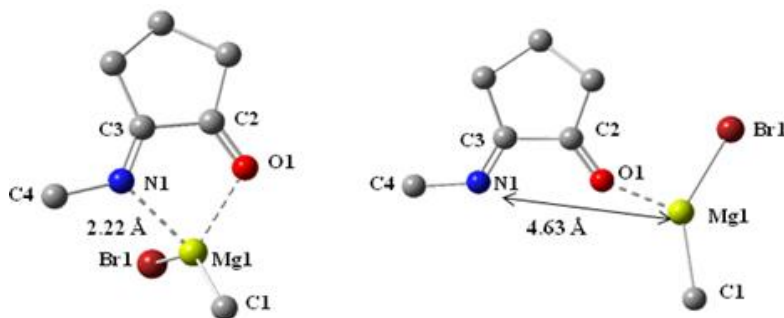


Figure 5: Chelated and non-chelated structures of Model system (Hydrogen atoms have been omitted for clarity).

On carrying out similar studies with the real system the interaction of Mg and N was preferred despite the sterically bulky 2, 6 dimethyl phenyl group at the imine nitrogen. The primary difference between the two structures was the reorientation of the phenyl group to facilitate the Mg-N coordination. The chelated structure (Mg1-N1=2.27 Å) was stabilized by -11.26 kcal/mol than the non-chelated model (Mg1-N13.99 Å) (Figure 6).

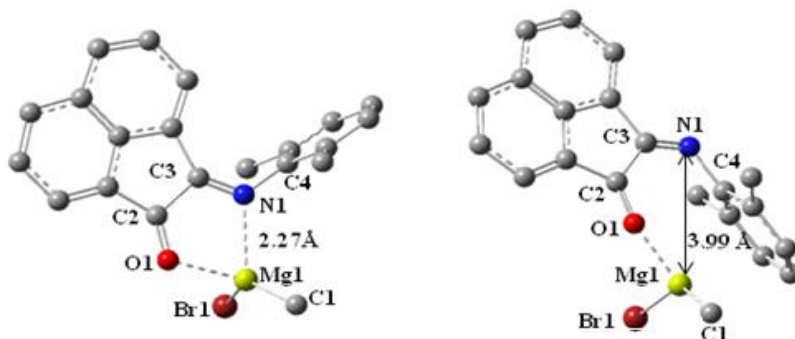


Figure 6: Chelated and non-chelated structures of Real system (Hydrogen atoms have been omitted for clarity).

1.4.3 Model System

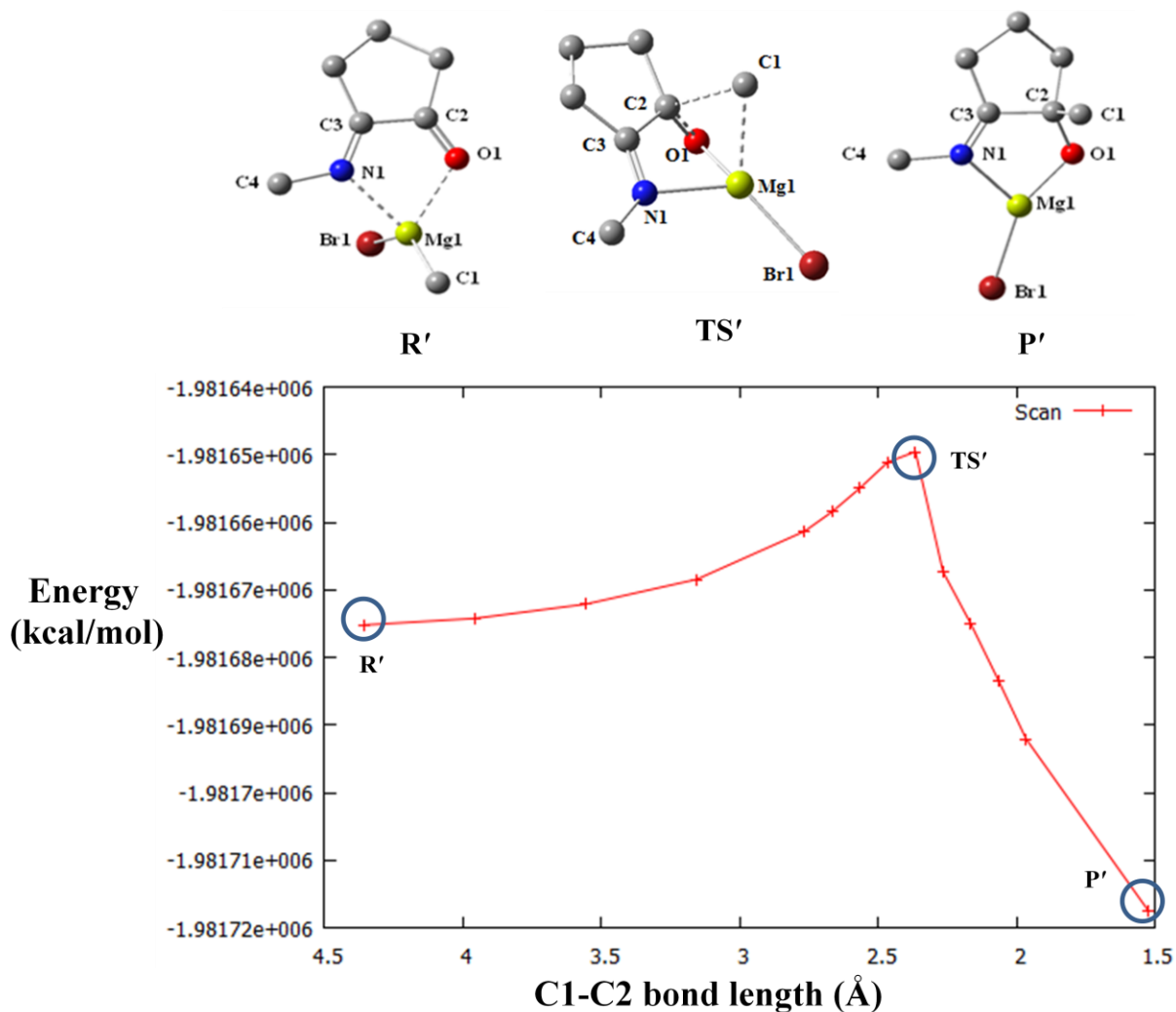


Figure 7: Plot of Energy (kcal/mol) vs C1-C2 bond length (Å) for model system.

The post-complex (**P'**) was stabilized by -23.99 kcal/mol compared to the pre-complex (**R'**). The carbonyl carbon and the methyl carbon of the Grignard reagent are at a distance of 4.36 Å (C1-C2) and 1.54 Å (C1-C2) in the pre-complex (**R'**) and post-complex (**P'**) respectively. Thus for locating the probable TS structure the carbonyl carbon and methyl carbon distance was scanned between this interval which lead to a high energy transition structure between the C1-C2 distances of 2.76 Å and 1.96 Å.

For further investigation this interval was scanned at intervals of 0.1 Å, and energetically a structure was maximized at C1-C2=2.36 Å from the scan plot, with the corresponding Mg1-N1 bond distance being 2.17 Å (Figure 7).

To get further insight into the transition structure we scanned our model system **2'** by varying both the C1-C2 and Mg1-N1 distance which resulted in a maxima in the potential energy surface at C1-C2 and Mg1-N1 bond distances being 2.36 Å and 2.21 Å respectively. Hence, we calculated the energies of the optimized structures by fixing the C1-C2 bond length at 2.36 Å and varying the Mg1-N1 distance between 2.17 Å and 2.21 Å at intervals of 0.1 Å. Finally we arrived at a transition state **TS'** (Figure 8) with C1-C2 bond distance at 2.36 Å and Mg1-N1 at 2.21 Å which was located 19.51 kcal/mol (Figure 9) above the pre-complex **R'**. The transition state obtained from QST2 calculations (18.75 kcal/mol above **R'**) was in close agreement with **TS'** both energetically and structurally. The C1-C2 (2.41 Å) and Mg1-N1 (2.18 Å) (Table 1) bond lengths in the predicted transition state using QST2 calculations showed only minor differences of 0.05 Å and 0.03 Å compared to **TS'**.

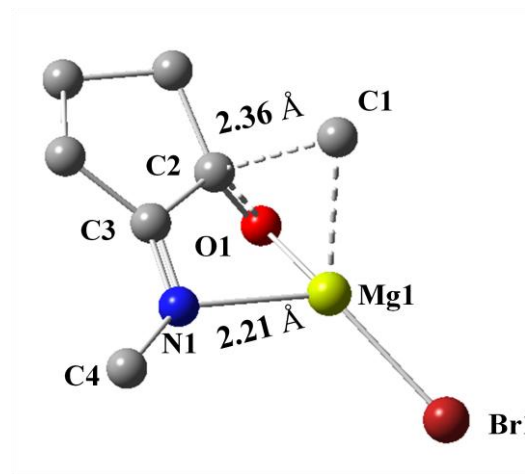


Figure 8: Transition State (**TS'**) for model system. (Hydrogen atoms have been omitted for clarity)

However on carrying out on scan and QST2 calculations using B3LYP/6-311+G(2d,p), we observed that both these methods predict almost the same transition state located 17.62 kcal/mol above the pre-complex. Even the structural parameters exhibit negligible deviations of 0.03 Å and 0.01 Å for the C1-C2 and Mg1-N1 bond lengths respectively.

Table 1: Selected bond lengths (Å) and angles (°) for model system transition states obtained by different methodologies

Bond Length(Å)/Angle (°)	Manual (HF/B3LYP) (TS=19.51 kcal/mol)	QST2 (HF/B3LYP) (TS=18.75 kcal/mol)	Manual (B3LYP/B3LYP) (TS=17.62 kcal/mol)	QST2 (B3LYP/B3LYP) (TS=17.62 kcal/mol)
C1-C2	2.36	2.41	2.46	2.49
Mg1-N1	2.21	2.18	2.19	2.20
C2-O1	1.27	1.26	1.25	1.25
C1-Mg1	2.31	2.27	2.28	2.26
Mg1-Br1	2.35	2.35	2.39	2.39
C2-C3	1.53	1.53	1.53	1.53
C3-N1	1.25	1.25	1.27	1.27
N1-C4	1.47	1.47	1.45	1.45
C2-C1-Mg1	60.75	61.16	59.49	59.75
C2-O1-Mg1	90.03	89.78	87.19	87.28
N1-Mg1-O1	81.84	81.62	82.25	81.74
N1-Mg1-Br1	121.72	120.31	123.75	122.76
C2-C3-N1	116.86	116.83	117.75	117.76

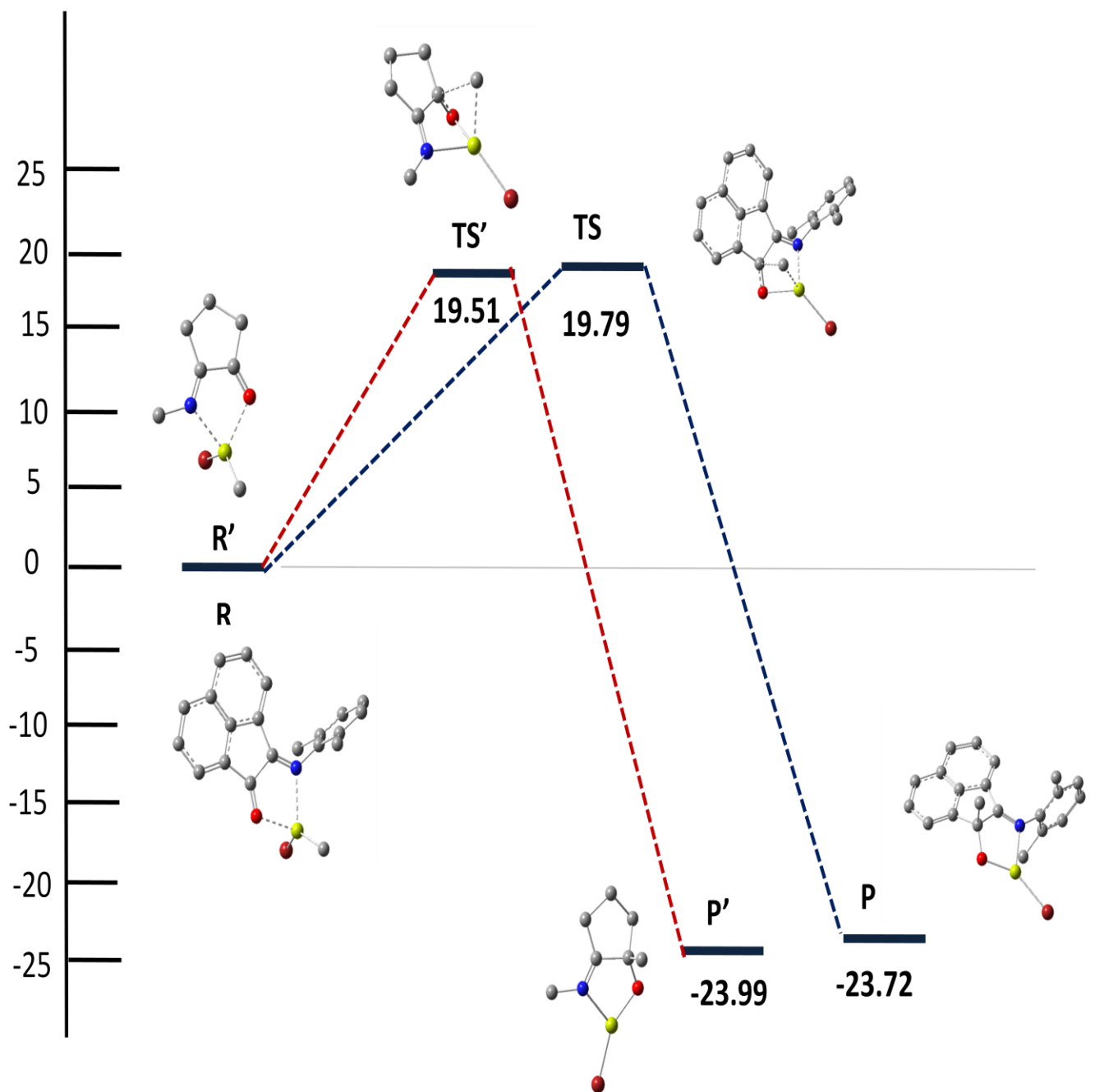


Figure 9: Energy profile of the model and real system (red and blue dotted lines represent the model and real system respectively), all energies are in kcal/mol.

As evident from the studies on the model system both the HF/B3LYP and the B3LYP/B3LYP method almost produce similar results. Thus to make the computations cost-effective we have restricted ourselves to the HF/B3LYP method while analyzing ligand **2**.

1.4.4 Real System

The post complex **P** is stabilized by an energy of -23.72 kcal/mol (Figure 9). From the variation of the C1-C2 bond length between 4.32 Å and 1.62 Å a high energy transition state was evident between 2.22 Å and 2.82 Å (Figure 10). On investigating this interval by varying the C1-C2 bond length by 0.1 Å we arrived at a transition state (**TS**) (Figure 11) located 19.79 kcal/mol above the pre-complex (**R**) with C1-C2 and Mg1-N1 distances being 2.42 Å and 2.21 Å respectively.

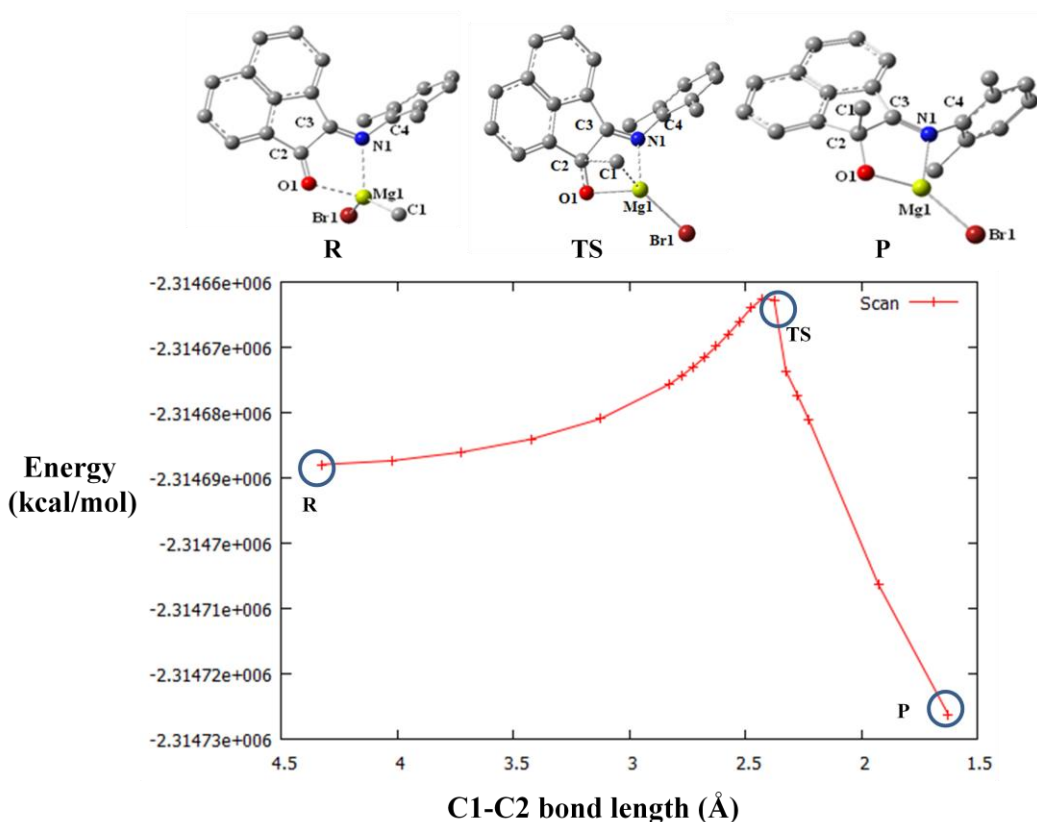


Figure 10: Plot of Energy (kcal/mol) versus carbonyl C and methyl C (C1-C2) distance (Å) for the real system.

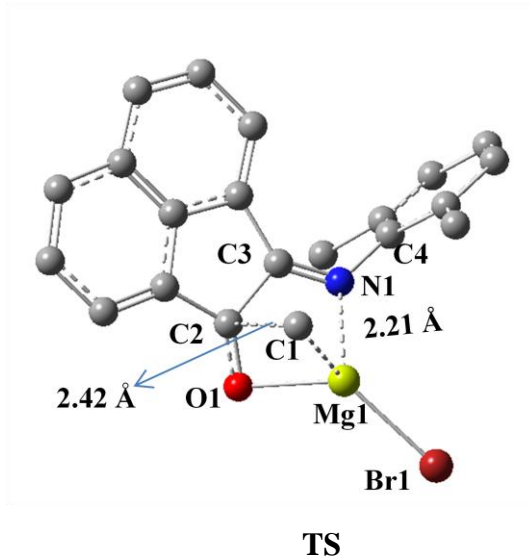


Figure 11: Transition state (TS) for real system (Hydrogen atoms have been omitted for clarity).

Transition state obtained by QST2 calculations was at energy of 16.73 kcal/mol compared to **R**. The C1-C2 bond lengths of 2.42 Å and 2.41 Å and Mg1-N1 bond lengths of 2.21 Å and 2.20 Å (Table 2) in the transition states obtained by scanning the C1-C2 bond and QST2 calculations respectively revealed structural similarities between the transition states obtained by the above two methods.

Table 2: Selected bond lengths (Å) and angles (°) for real system transition states obtained by different methodologies:

Bond Length(Å)/Angle (°)	Manual (HF/B3LYP) (TS=19.79 kcal/mol)	QST2 (HF/B3LYP) (TS=16.73 kcal/mol)
C1-C2	2.42	2.41
Mg1-N1	2.21	2.20
C2-O1	1.24	1.25
C1-Mg1	2.22	2.26
Mg1-Br1	2.35	2.35
C2-C3	1.55	1.55
C3-N1	1.26	1.26
N1-C4	1.44	1.44

C2-C1-Mg1	62.67	61.38
C2-O1-Mg1	90.22	89.48
N1-Mg1-O1	80.94	81.88
N1-Mg1-Br1	122.67	123.82
C2-C3-N1	116.82	116.89

The energy difference of approximately 3kcal/mol can be attributed to the deviation of the Mg1-C1 bond by 0.04 Å in the obtained transition states by the two methods. The deviation though apparently small, has a significant impact on the energy as in the course of the reaction the Mg1-C1 bond is broken to form the C1-C2 bond.

1.5 Conclusion

Thus modeling the transition state, gave us an elaborate insight into the mechanistic aspects of Grignard reaction with Ar-BIAO ligands. The spontaneous and exothermic nature of the reaction is evident from the high stability of approximately 24 kcal/mol for the post-complex (**P**). Furthermore we arrive at an excellent understanding of the coordination environment of magnesium. From the theoretical analysis we can conclude that the reaction initiated with both nitrogen and oxygen simultaneously coordinating to magnesium to form a five-membered ring. The intramolecular chelation facilitated by the reorientation of the aryl group at the imine nitrogen was similar to the coordination of Ar-BIAO complexes with cobalt previously reported by our group.

References

- [1] For the presentation speech of Francois Auguste Victor Grignard's 1912 Nobel prize, see: <http://www.nobel.se/chemistry/laureates/1912/press.html>.
- [2] R. Fu., J. L. Ye, J. X. Dai, Y. P. Ruan and P. Q. Huang, *J. Org. Chem.*, 2010, **75**, 4230-42343.
- [3] M. Hatano, O. Ito, S. Suzuki and K. Ishihara, *J. Org. Chem.*, 2010, **75**, 5008-5016.
- [4] D. Seyferth, *Organometallics*, 2009, **28**, 1598-1605.
- [5] V. Schulze, P. G. Nell, A. Burtan and R.W. Hoffman, *J. Org. Chem.*, 2002, **68**, 4546-4548.
- [6] S. Yamazaki and S. Yamabe, *J. Org. Chem.*, 2002, **67**, 9346-9353.
- [7] G. E. Parris and E. C. Ashby, *J. Am. Chem. Soc.*, 1971, **93**, 1206-1213.
- [8] L. J. Guggenberger and R. E. Rundle, *J. Am. Chem. Soc.*, 1968, **90**, 5375-5378.
- [9] A. M. Henriques and A. G. H. Barbosa, *J. Phys. Chem. A.*, 2011, **115**, 12259-12270.
- [10] H. Lioe, J. M. White and R. A. J. O'Hair, *J. Mol. Model.*, 2011, **17**, 1325-1334.
- [11] F.A.Cram and F.A.A.Elhafez, *J. Am. Chem. Soc.*, 1952, **74**, 582.
- [12] V. S. Safont, V. Moliner, M. Oliva, R. Castillo, J. Andres, F. Gonzalez and M. Carda, *J. Org. Chem.*, 1996, **61**, 3467.
- [13] R. J. Smith, M. Trzoss, M. Bühl and S. Bienz, *Eur. J. Org. Chem.*, 2002, **16**, 2770-2775.
- [14] J. L. Ye, P. Q. Huang and X. Lu, *J. Org. Chem.*, 2007, **72**, 35-42.
- [15] S. Anga, M. Paul, K. Naktode, R. K. Kottalanka and T. K. Panda, *Z. Anorg. Allg. Chem.*, 2012, **638**, 1311-1315.
- [16] J. Kovach, M. Peralta, W. W. Brennessel and W. D. Jones, *J. Mol. Struct.*, 2011, **992**, 33-38.
- [17] a) M. Jeon, C. J. Han and S. Y. Kim, *Macromol. Res.*, 2006, **14**, 306-311; b) B. L. Small, R. Rios, E. R. Fernandez, D. L. Gerlach, J. Halfen and M. J. Carney, *Organometallics*, 2010, **29**, 6723-6731; c) B. M. Schmiege, M. J. Carney, B. L. Small, D. L. Gerlach, and J. A. Halfen, *Dalton Trans.*, 2007, 2547-2562.
- [18] Unpublished Results by our group
- [19] P. Hohenberg and W. Kohn, *Phys. Rev. B.*, 1969, **136**, 864.
- [20] Gaussian 09, Revision B.01, M. J. Frisch, G. W. Trucks, H. B. Schlegel, G. E. Scuseria, M. A. Robb, J. R. Cheeseman, G. Scalmani, V. Barone, B. Mennucci, G. A. Petersson, H. Nakatsuji, M. Caricato, X. Li, H. P. Hratchian, A. F. Izmaylov, J. Bloino, G. Zheng, J. L. Sonnenberg, M.

Hada, M. Ehara, K. Toyota, R. Fukuda, J. Hasegawa, M. Ishida, T. Nakajima, Y. Honda, O. Kitao, H. Nakai, T. Vreven, J. A. Montgomery, Jr., J. E. Peralta, F. Ogliaro, M. Bearpark, J. J. Heyd, E. Brothers, K. N. Kudin, V. N. Staroverov, T. Keith, R. Kobayashi, J. Normand, K. Raghavachari, A. Rendell, J. C. Burant, S. S. Iyengar, J. Tomasi, M. Cossi, N. Rega, J. M. Millam, M. Klene, J. E. Knox, J. B. Cross, V. Bakken, C. Adamo, J. Jaramillo, R. Gomperts, R. E. Stratmann, O. Yazyev, A. J. Austin, R. Cammi, C. Pomelli, J. W. Ochterski, R. L. Martin, K. Morokuma, V. G. Zakrzewski, G. A. Voth, P. Salvador, J.J. Dannenberg, S. Dapprich, A. D. Daniels, O. Farkas, J. B. Foresman, J. V. Ortiz, J. Cioslowski, and D. J. Fox Gaussian, Inc., Wallingford CT, 2010.

[21] GaussView, Version 5, Roy Dennington, Todd Keith and John Millam, *Semichem Inc.*, Shawnee 539 Mission KS, 2009.

[22] C. Peng, P. Y. Ayala, H. B. Schlegel, and M. J. Frisch, *J. Comp. Chem.*, 1996, **17**, 49.

[23] Peng and H. B. Schlegel, *Israel J. Chem.*, 1994, **33**, 449.

[24] a) D. Becke, *J. Chem. Phys.*, 1993, **98**, 5648; b) C. Lee, W. Yan and R. G. Parr, *Phys. Rev. B*. 1988, **37**, 785.

[25] J.B. Foresman and T. M. Frisch, *Exploring Chemistry with Electronic Structure Methods*, Second 543 Edition, Gaussian, Inc. Pittsburgh, PA.

Chapter 2

Basicity of *Imidazolin-2-ylidene-1,1-diphenylphosphinamine* and Analogous Systems-A Computational Study

2.1 Introduction

N-heterocyclic imines of the imidazolin-2-ylidene¹ type has found several widespread applications in the fields of homogeneous catalysis², material science³ and medicinal chemistry⁴. The enhanced stability of these carbenes is due to the presence of the imidazolium ring which can effectively stabilize a positive charge. As result these ligands are highly basic in nature with strong electron donating capacity towards early transition metals and metals in high oxidation state⁵. Besides several rare earth metal complexes supported by imidazolin-2-iminato ligands have also been reported⁶. Imidazolin-2-imines are a fascinating class of ligands bearing pseudo-isolobal analogy with cyclopentadienyl ligands. The versatility of these ligands arises due to their potential to act 2σ , 2π - as well as 2σ , 4π -electron donors⁷. The imidazolin-2-imine ligand has been extended by our group to synthesize imidazolin-2-ylidene-1,1-diphenylphosphinamine and its chalcogenide derivatives (O, S, Se, Te) (Figure 1).

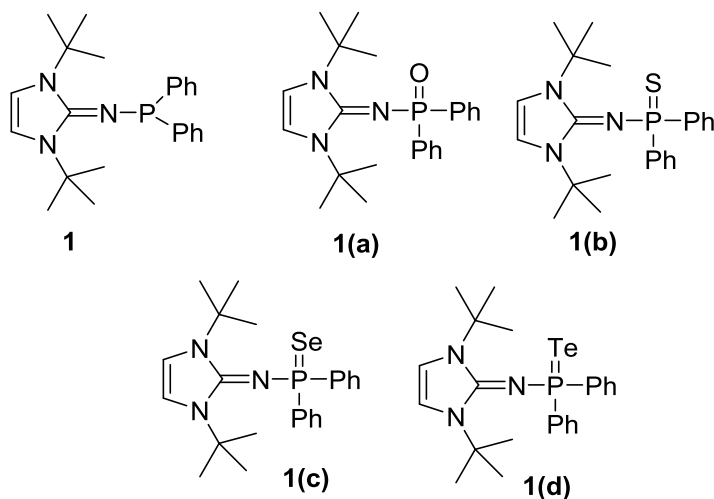
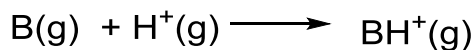


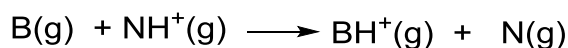
Figure 1: imidazolin-2-ylidene-1,1-diphenylphosphinamine and corresponding chalcogenides

Protonation plays an important role in several branches of chemistry including atmospheric and biochemistry⁸. Proton affinities, protonation energies and gas phase basicities are some of the important parameters used to judge a compound or atom's capability to accept a proton in the gas phase⁹.



Equation 1

Proton affinity (PA) is defined as $-\Delta H$ of the reaction (1). The Gibbs Free Energy of the above reaction (1) is defined as the gas phase basicity. There are quite a few techniques to experimentally measure the PA of a compound. For example mass and ion mobility spectrometry (IMS) that can be used to measure the proton affinity of B from the gas phase reaction **2**¹⁰.



Equation 2

But experimental measurement of PA remains quite a complicated procedure. Thus recently there have been quite a lot of efforts to calculate PA through computational methods¹¹.

Previously our group being interested in the computational study of Phosphorus-Nitrogen systems reported DFT studies on the addition of BH_3 to these systems. Furthermore *Tamm et al.*¹² reported the basicity calculations of imidazolin-2-imine class of ligands. Herein we were interested to investigate computationally the basicity of *Imidazolin-2-ylidene-1,1-diphenylphosphinamine* and analogous ligands, since addition of the diphenyl phosphine group on the exocyclic nitrogen will have a marked effect on the basicity due to delocalisation of the lone pair of electrons on nitrogen into the vacant *d* orbital of phosphorus ($\text{N}(\text{p}\pi)\text{-P}(\text{d}\pi)$ bonding)¹³.

2.2 Scope of the work

Study of ligand basicity can help to predict a ligand's reactivity towards stabilizing electron deficient transition metal as well as lanthanide complexes. Thus here we are interested to study the basicity of the synthesized ligand **1** (*1,3-di-tert-butyl-N-(diphenylphosphino)-1H-imidazol-2(3H)-imine*) and compare it with the model systems **1'** (*1,3-di-tert-butyl N(diphenylphosphino)imidazolin-2-imine*) and **1''**(*1,3-di-tert-butyl-1-3-dimethyl-2(diphenylphosphino)guanidine*) using density functional calculations. Investigation of the protonation energies and the NBO charges would help us get a better insight not only towards the ligand basicity but also judge the stabilization of the positive charge by the imidazolin ring. Also to explore the changes in the electronic environment around the exocyclic nitrogen , with different chalcogens bonded to phosphorus, protonation energy and NBO analysis were carried out on **1(a)**, **1(b)** and **1(c)**.

2.3 Methodology

The computational methodology used has already been discussed in the previous chapter. The enhanced basicity and nucleophilicity of imidazoline-2-imine systems due to the negative charge on the exocyclic nitrogen atom; the introduction of P-N bond to the ligands favours the delocalization of the nitrogen lone pairs into the vacant *d* orbital of phosphorus atom. Study of ligand basicity can help to predict a ligand's reactivity towards stabilizing electron deficient chemical entities. Thus here we are interested to study the basicity of the synthesized ligand **1** (*1,3-di-tert-butyl-N-(diphenylphosphino)-1H-imidazol-2(3H)-imine*) and compare it with the model systems **1'** (*1,3-di-tert-butyl- N(diphenylphosphino)imidazolin-2-imine*) and **1''** (*1,3-di-tert-butyl-1,3-dimethyl-2-(diphenylphosphino)guanidine*) (Figure 2), using computational methods.

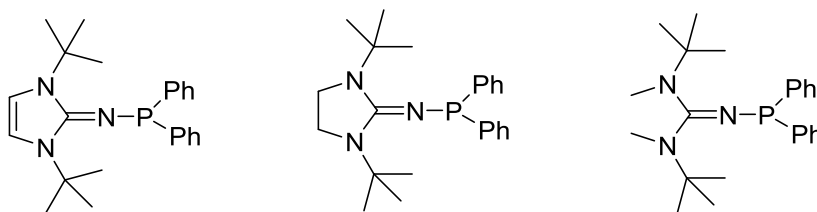


Figure 2: Synthesized ligand **1** and model systems **1'** and **1''**.

Synthesized ligand **1** contains the imidazoline ring which is absent in the model systems **1'** and **1''**. Thus it helps us to infer the effect of the imidazoline ring on the basicity of a system, by comparing with the two model systems. Furthermore the systems are chosen in such a way that we can make a comparative study as we go from the cyclic to acyclic analogue. Earlier studies¹² emphasized the importance of protonation energy and charge on exocyclic nitrogen atom for prediction of basicity of these type of ligands. We have calculated the protonation energy¹⁴ of the ligands and the Natural Bond Order (NBO) charge on the nitrogen atom for the better understanding of reactivity of entities.

Protonation energy was calculated as follows: $B + H^+ \rightleftharpoons BH^+$

Equation 3

$$\text{Protonation Energy [PE (B)]} = E(H^+) + E(B) - E(BH^+)$$

Computational analysis have also been carried out on the chalcogenides of ligand **1** with the aim to make a comparative study of the basicity of ligands **1(a)**, **1(b)** and **1(c)** with the changing electronegativity of the chalcogens.

2.4 Results and Discussion:

The ligand **1** was freely optimized without any geometrical constraints and the optimized structure was in good agreement with that established by X-ray diffraction. The bond lengths N3-C1 (1.396 Å) and N2-C4 (1.489 Å) are in close agreement with the experimental values (1.396 Å and 1.490 Å). The bond angles C3-C2-N2 (108.25°) and C2-N2-C1 (109.68°) are in good agreement with the experimental structure (108.02° and 109.68° (109.32°)). However the bond angle C1-N1-P1 (145.67 °) showed a significant deviation of 7.65° from the experimental value (138.02°) (Figure 3).

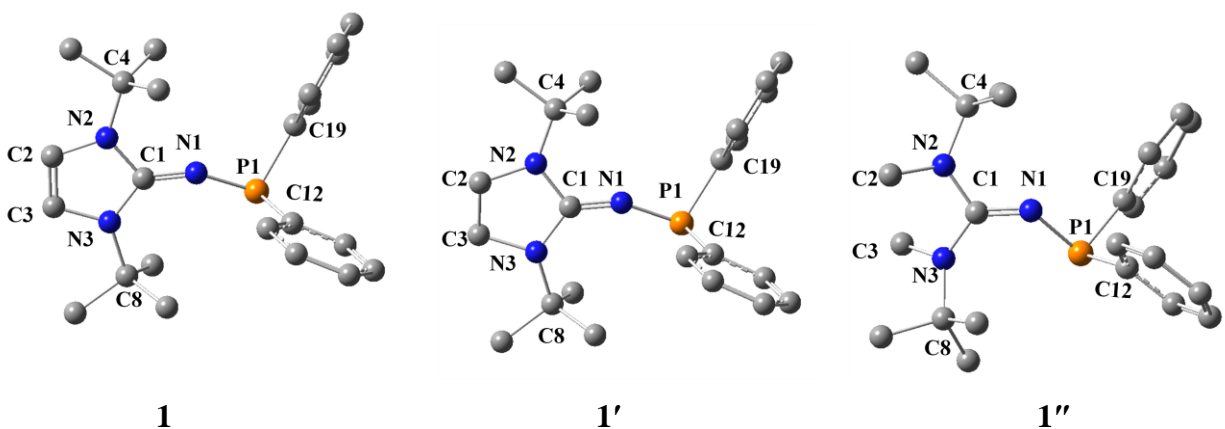


Figure 3: Optimized structures of ligand **1**, **1'** and **1''** using HF 3-21G(d) (Hydrogen atoms have been omitted for clarity).

Thus for further investigation ligands **1**, **1'** and **1''** were optimized using density functional theory calculations (B3LYP 6-311+G(2d,p)). The optimized structure so obtained was in excellent agreement with experimental one, as the deviation in the bond angle of C1-N1-P1 (136.19°) was reduced to 1.83°. In the DFT optimized structure other bond angles and lengths were also very close to the experimental values. . The calculated bond lengths P1-C19 (1.864 Å) and N2-C2 (1.385 Å) matched with the experimental values (1.861 Å and 1.389 Å). The theoretical bond angles C3-N3-C1 (108.67°) and C1-N1-P1 (136.19°) are also in good agreement

with the experimental structure (108.52° and 138.02°). The optimized structures **1** and **1'** are geometrically close whereas **1''** shows distinct differences in bond angles and lengths compared to **1** and **1'**. This feature is clearly reflected in the bond angle C1-N1-P1 which is 145.67° and 149.35° for ligands **2** and **2'** in the HF optimized structure, but drastically reduces to 129.37° in ligand **1''**. Similar trend is observed in the B3LYP optimized structures where the C1-N1-P1 bond angles are 136.19°, 140.78° and 124.25° for ligands **1**, **1'** and **1''** respectively. Comparison of all the computed structural parameters with experimental data for ligand **1** are shown in Table 1.

Table 1: Selected bond lengths [Å] and angles[°] of ligand **1** by different methodologies

Bond Length[Å]/angle[°]	Experiment	HF 3-21G*	B3LYP 6-311+G(2d,p)
P1-N1	1.644	1.654	1.682
P1-C12	1.845	1.839	1.855
P1-C19	1.861	1.841	1.864
N3-C3	1.389	1.401	1.394
N3-C1	1.396	1.396	1.408
N3-C8	1.495	1.492	1.501
N2-C2	1.389	1.397	1.385
N2-C1	1.395	1.389	1.399
N2-C4	1.49	1.489	1.496
N1-C1	1.295	1.275	1.294
C2-C3	1.295	1.322	1.34
N1-P1-C12	101.35	102.29	101.82
N1-P1-C19	101.6	102.95	101.82
C12-P1-C19	97.65	98.89	98.95
C3-N3-C1	108.52	108.79	108.67
C3-N3-C8	123.42	123.06	122.36
C1-N3-C8	127.82	128.12	128.98
C2-N2-C1	109.32	109.68	109.69
C2-N2-C4	125.12	125.16	124.8

C1-N2-C4	125.62	125.13	125.49
C1-N1-P1	138.02	145.67	136.19
N3-C1-N2	121.2	122.78	121.37
N3-C1-N1	133.62	132.43	133.9
N2-C1-N3	104.95	104.76	104.64
C3-C2-N2	108.02	108.25	108.22

The calculated geometries of **4** and **5** (Figure 4) by B3LYP/6-311+G(2d,p) were in excellent agreement to that of structural parameters obtained by X-ray diffraction. Furthermore on comparing the optimized structures of **3**, **4** and **5** we see that there occurs a increase in the P-X (X=O,S,Se) bond length 1.50 Å (**3**), 1.99 Å(**4**), 2.15 Å (**5**) (Table 2) , which is expected from the increase in size of the chalcogens. Most of the other bond lengths and angles are similar for the three chalcogenides except the C1-N1-P1 angle. C1-N1-P1 angles for **4** (133.8°) and **5** (133.79°) are almost identical, while for **3** (143.2°) deviates by approximately 10°.

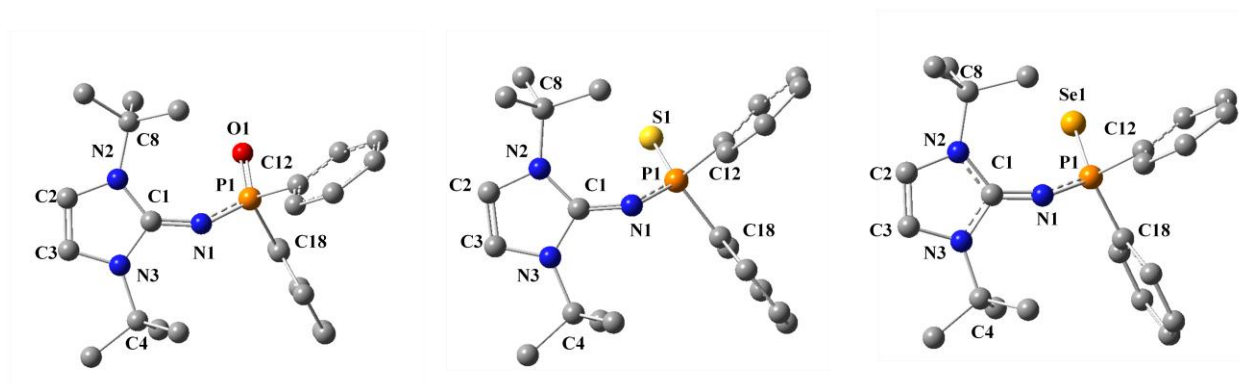


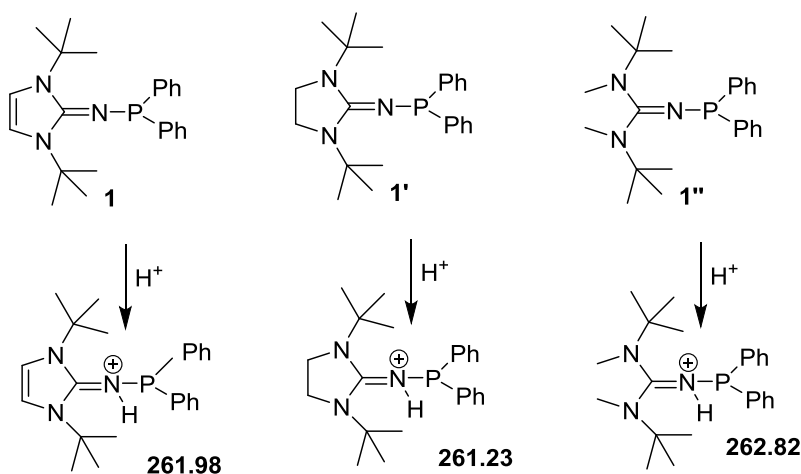
Figure 3: Optimized structures of **3**, **4** and **5** by B3LYP/6-311+G(2d,p)

Table 2: Selected bond lengths (Å) and angles (°) from the calculated geometries of **3**, **4** and **5** by B3LYP/6-311+G(2d,p) (Experimental values are given in brackets alongside).

Bond Length[Å]/angle[°]	3	4	5
P1-N1	1.62	1.62(1.60)	1.63(1.61)
O1-P1	1.50	-	-
S1-P1	-	1.99(1.96)	-
Se1-P1	-	-	2.15(2.12)
P1-C12	1.83	1.84(1.83)	1.84(1.83)
P1-C18	1.83	1.85(1.83)	1.85(1.83)
N1-C1	1.30	1.31(1.33)	1.31(1.33)
N3-C1	1.39	1.39(1.37)	1.39(1.38)
N3-C4	1.50	1.50(1.50)	1.50(1.50)
N2-C2	1.39	1.39(1.38)	1.39(1.39)
N2-C1	1.39	1.39(1.37)	1.39(1.37)
N2-C8	1.51	1.51(1.50)	1.51(1.50)
C2-C3	1.34	1.34 (1.34)	1.34(1.33)
N1-P1-C12	104.72	105.03(106.63)	105.30(105.68)
N1-P1-C18	106.64	107.30(105.81)	107.72(106.95)
C12-P1-C18	103.91	100.48(101.19)	100.02(101.28)
O1-P1-C12	111.21	-	-
S1-P1-C12	-	112.96(111.73)	-
Se1-P1-C12	-	-	112.97(111.73)
O1-P1-C18	108.38	-	-
S1-P1-C18	-	110.30(110.64)	-
Se1-P1-C18	-	-	110.55(110.64)
O1-P1-N1	120.67	-	-
S1-P1-N1	-	119.02(119.12)	-
Se1-P1-N1	-	-	118.54(118.97)
C3-N3-C1	109.33	109.33(108.90)	109.32(109.20)

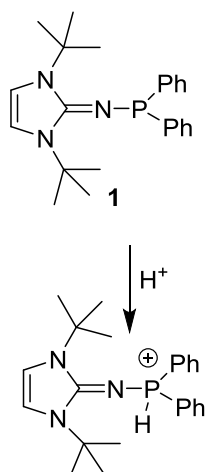
C3-N3-C4	124.47	123.81(123.61)	123.67(127.23)
C2-N2-C1	108.56	108.74(109.20)	108.77(108.89)
C2-N2-C8	121.60	118.40(124.26)	118.22(123.71)
C1-N1-P1	143.20	133.86(130.90)	133.79(130.72)
N3-C1-N2	105.32	105.25(105.93)	105.30(105.72)
N3-C1-N1	122.88	124.26(127.90)	124.59(126.23)
N2-C1-N1	131.68	130.39(125.98)	130.01(127.82)

Scheme 1 depicts the protonation of three ligands at nitrogen. The energies have been calculated using only B3LYP method without including thermal correction; the difference between these two methods is approximately 10 kcal/mol, and there is no change in trend towards being protonated.



Scheme 1: Protonation of synthesized ligand **1** and model systems **1'** and **1''**.

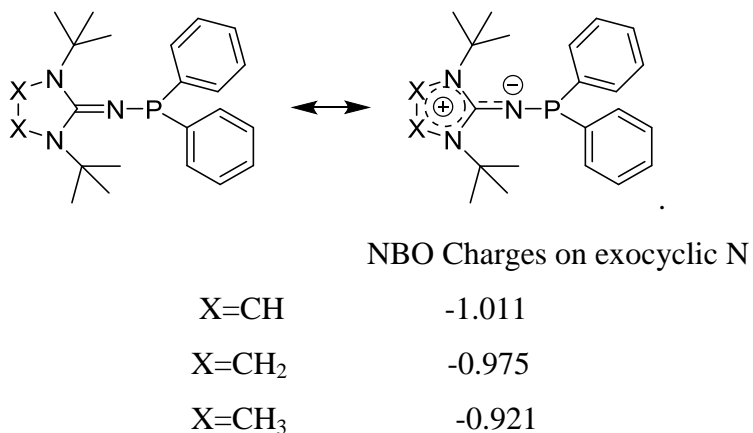
On protonation of the ligands, the exocyclic nitrogen is most probable to pick up the proton than phosphorous, where the protonation energy of **1** is 248.05 as compared to 252.88 kcal/mol (Scheme 2).



Scheme 2: Protonation of phosphorus

Our calculations only reveal a slight difference in the protonation energies between three compounds. *Tamm et al* ^[12] reported that protonation affinities were not the best descriptors of basicity. From the calculated protonation energies we can infer that these are inconclusive in comparing the basicity of the three systems.

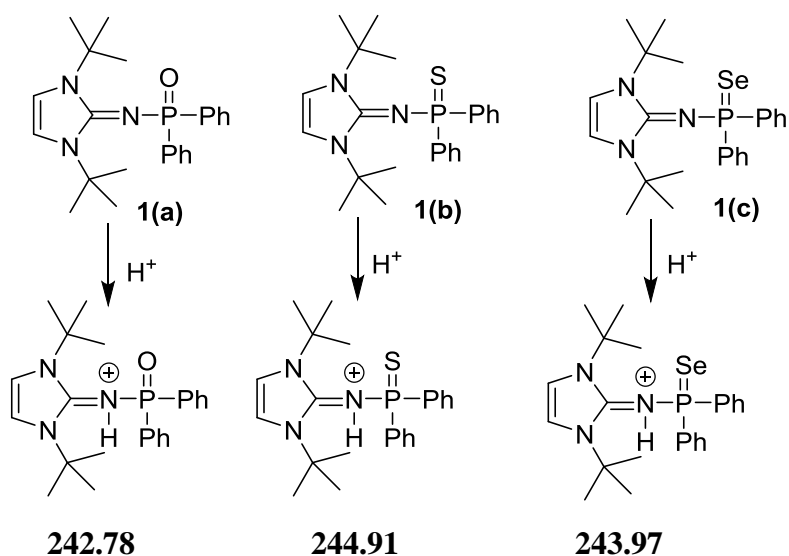
Furthermore on calculating the NBO charges on ligand **1** the nitrogens on the imidazole ring have charges of -0.0458 and -0.469; the exocyclic nitrogen has a charge of -1.011, whereas the phosphorus has a charge of +1.024. Thus the exocyclic nitrogen having the highest negative charge is most likely to get protonated. Thus NBO charges on the exocyclic nitrogen were also calculated at DFT level (B3LYP/6-311+G(2d,p)). A pronounced difference was found between **1**(-1.011), its saturated analogue **1'** (-0.975) and acyclic **1''** (0.921). Hence the NBO charges clearly indicate that ligand **1** is more basic compared to model systems **1'** and **1''**.



Scheme 3: Calculated NBO charges on exocyclic Nitrogen for ligand **1** and model systems **1'** and **1''**.

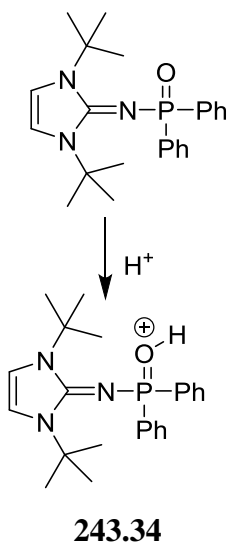
The higher negative charge on exocyclic nitrogen of **1** can be attributed to the stabilization of the zwitterionic form by the imidazolin ring.

Thereafter we decided to computationally explore the chalcogenides **1(a)**, **1(b)** and **1(c)**. The NBO charges on the exocyclic nitrogen for **1a**, **1b** and **1c** are -1.075, -1.076 and -1.087 respectively. For the sulphur and selenide derivative the chalcogens have a charge of -0.642 and -0.591 respectively and thus the exocyclic nitrogen having the highest negative charge is most likely to get protonated and we calculated the corresponding protonation energies (by the combined method) which were 244.91 kcal/mol and 243.97 kcal/mol respectively (Scheme 4).



Scheme 4: Protonation of **1(a)**, **1(b)** and **1(c)** . Energies are reported in kcal/mol.

However for the oxygen derivative (**1(a)**) oxygen has a higher negative charge (-1.139) than exocyclic nitrogen (-1.075). Protonation at oxygen (Scheme 5) lead to a protonation energy (243.34 kcal/mol) approximately 0.6 kcal/mol higher than the protonated form where exocyclic nitrogen bears the H⁺. Thus while the protonation energies does not always give a clear idea, the NBO analysis clearly indicate that for **1(a)** the more electronegative oxygen is likely to get protonated.



Scheme 5: Protonation at oxygen for **1(a)**. Energies are reported in kcal/mol.

The NBO charges were also calculated using B3LYP method and a similar trend was observed. For **1(a)** oxygen had a higher negative charge (-1.130) as compared to exocyclic nitrogen (-1.077). From Table 3 it is evident that occurs a decrease on the negative charge on exocyclic nitrogen (-1.077, -1.090 and -1.095 for **1(a)**,**1(b)** and **1(c)** respectively)as we go from oxygen to selenium, thus there occurs a decrease in the tendency of the exocyclic nitrogen to accept a proton, as the electronegativity of the chalcogenide bonded to phosphorus increases.

Table 3: Charge distribution in **1(a)**, **1(b)** and **1(c)**.

Ligand	Chalcogenide	HF/B3LYP		B3LYP/B3LYP	
		Charges on exocyclic N atom	Charge on chalcogenide	Charges on exocyclic N atom	Charge on chalcogenide
1(a)	O	-1.075	-1.139	-1.077	-1.130
1(b)	S	-1.076	-0.642	-1.090	-0.653
1(c)	Se	-1.087	-0.591	-1.095	-0.593

2.5 Conclusion

In summary, the structure of the previously synthesized ligand *1,3-di-tert-butyl-N-(diphenylphosphino)-1H-imidazol-2(3H)-imine* and its corresponding sulphur and selenium derivative has been optimized and the optimized structure is in close agreement with the experimental one. Besides, two other model systems **1'** and **1''** analogous to **1** have been optimized. For all the three structures protonation energies and NBO charges have been calculated as parameters for quantifying basicity. From the NBO charges it was quite evident that the exocyclic nitrogen having the highest negative charge is most likely to get protonated. Furthermore, it has been observed that there occurs a decrease in basicity as we go from the cyclic to the acyclic analogue. Also the electronic structure around the exocyclic nitrogen has been probed with different chalcogenides bonded to phosphorus and it has been observed that there occurs a decrease in the basicity with the increasing electronegativity of the chalcogenides.

References:

- [1] (a) M. Regitz, *Angew. Chem. Int. Ed.*, 1996, **35**, 725–728; (b) A. J. Arduengo, III and R. Krafczyk, *Chem. Unserer Zeit*, 1998, **32**, 6–14; (c) V. Nair, S. Bindu and V. Sreekumar, *Angew. Chem. Int. Ed.*, 2004, **43**, 5130–5135.
- [2] T. Weskamp, V. P. W. Böhm and W. A. Herrmann, *J. Organomet. Chem.*, 2000, **600**, 12–22.
- [3] A. J. Boydston, K. A. Williams and C. W. Bielawski, *J. Am. Chem. Soc.*, 2005, **127**, 12496–12497.
- [4] J. C. Garrison and W. C. Youngs, *Chem. Rev.*, 2005, **105**, 3978–4008.
- [5] K. Dehnicke and F. Wellerm, *Coord. Chem. Rev.*, 1997, **158**, 103.
- [6] X. Wu and M. Tamm, *Coord. Chem. Rev.*, 2014, **260**, 116–138.
- [7] D. W. Stephan, *Organometallics*, 2005, **24**, 2548–2560.
- [8] C. Biot, R. Wintjens and M. Rooman, *J. Am. Chem. Soc.*, 2004, **126**, 6220.
- [9] Y. Valadbeigi and H. Farrokhpour, *Int. J. Quant. Chem.*, 2013, **113**, 1717–1721.
- [10] M. Tabrizchi and S. Shooshtari, *J. Chem. Thermodyn.*, 2003, **35**, 863.
- [11] M. Namazian and M. L. Coote, *J. Chem. Thermodyn.*, 2008, **40**, 1116.
- [12] M. Tamm, D. Petrovic, S. Randoll, S. Beer, T. Bnnenberg, P. G. and J. Grunenberg, *Org. Biomol. Chem.*, 2007, **5**, 523–530.
- [13] D. Grec, L. G. Hubert-Pfzgraf, A. Grand and J. G. Riess, *J. Am. Chem. Soc.*, 1980, **102**, 7134.
- [14] I. A. Koppel, R. Schwesinger, T. Breuer, P. Burk, K. Herodes, I. Koppel, I. Leito and M. Mishima, *J. Phys. Chem.*, 2001, **105**, 9575–9586.

Curriculum Vitae

Name: Sayak Das Gupta

Date of Birth: 5th March, 1991

Marital Status: Single

Contact no: 09640213853

Sex: Male

Email id: sayakd4@gmail.com

Nationality: Indian

➤ **Academic Background:**

Degree	Institution	University/Board	Year of Passing	CGPA/Marks
M.Sc. in Chemistry	IIT Hyderabad	-	2014	9.56 (upto 3 rd Sem)
B.Sc. in Chemistry	St. Xavier's College, Kolkata	Autonomous under the University of Calcutta	2012	77.30%
ISC	St. Joseph's College, Kolkata	<u>Council for the Indian School Certificate Examinations</u>	2009	95.75 %
ICSE	St. Joseph's College, Kolkata	<u>Council for the Indian School Certificate Examinations</u>	2007	94.60 %

➤ **Awards and Honours:**

- Secured an All India Rank of 43 in GATE, 2014.
- Received "Award for Academic Excellence" in 2014 at IIT Hyderabad.
- Cleared CSIR-NET (JRF) in June 2013 with an All India Rank of 34.
- Secured a rank of 228 in Joint Admission Test for M.Sc. (JAM) in 2009.

➤ **Publications**

- Kishor Naktode, Jayeeta Bhattacharjee, Sayak Das Gupta, Hari Pada Nayek, Bhabani S. Mallik, and Tarun K. Panda "Unprecedented Calcium Metalla-macrocyclic Having Phosphinoselenoic Amide and Diphenylphosphinate in the Coordination Sphere" *Z. Anorg. Allg. Chem.*, **2014**, 640, 994-999.
- Kishor Naktode, Sayak Das Gupta, Jayeeta Bhattacharjee, Salil K. Jana, Hari Pada Nayek, Bhabani S. Mallik, and Tarun K. Panda "Functionalisation of Imidazolin-2-imine to Corresponding Phosphinamine, Chalcogenide (O, S, Se, Te) and Borane Compounds", **2014**, *submitted*.